



**HAL**  
open science

## Incremental Capacity Analysis as a diagnostic method applied to second life Li-ion batteries

Lucas Albuquerque, Fabien Lacressonnière, Xavier Roboam, Christophe  
Forgez

► **To cite this version:**

Lucas Albuquerque, Fabien Lacressonnière, Xavier Roboam, Christophe Forgez. Incremental Capacity Analysis as a diagnostic method applied to second life Li-ion batteries. ELECTRIMACS 2022, 14th International Conference of the International Association for Mathematics and Computer in Simulation, May 2022, Nancy, France. pp.451-463, 10.1007/978-3-031-24837-5\_34 . hal-03673979

**HAL Id: hal-03673979**

**<https://ut3-toulouseinp.hal.science/hal-03673979>**

Submitted on 20 May 2022

**HAL** is a multi-disciplinary open access archive for the deposit and dissemination of scientific research documents, whether they are published or not. The documents may come from teaching and research institutions in France or abroad, or from public or private research centers.

L'archive ouverte pluridisciplinaire **HAL**, est destinée au dépôt et à la diffusion de documents scientifiques de niveau recherche, publiés ou non, émanant des établissements d'enseignement et de recherche français ou étrangers, des laboratoires publics ou privés.

# Incremental Capacity Analysis as a diagnostic method applied to second life Li-ion batteries

Lucas Albuquerque · Fabien Lacressonnière · Xavier Roboam · Christophe Forgez

**Abstract** This work is inserted in the context of second life Li-ion batteries: for such storage devices, their first life characteristics are unknown and a simple capacity measurement might not be sufficient to fully characterize and get it ready for its second life. The Incremental Capacity Analysis (ICA) was used in this study to give a more intimate diagnosis of the batteries' Degradation Modes (DMs), providing a link with physical degradation phenomena. This method was applied to a lithium-ion battery module (NMC/Graphite) which was used in an electrical vehicle and to a single cell from a similar module in order to verify its potential use in this context. Both IC curves were then compared to a DM simulation using the *'Alawa* software, capable of simulating different ageing phenomena and their effects on the IC curves. Moreover, this work gives an intrinsic view and explanation of the IC signature for the mentioned battery technology.

## 1 Introduction

The increasing number of batteries produced and consumed nowadays can be attributed to the rise of electric vehicles (EVs) into the market. However, this step towards transport decarbonization created a problem of its own: what to do with these batteries after they are not suitable anymore to power said EVs? The answer to this question is either recycling or ending up in a landfill, creating another environ-

mental problem in itself. Nonetheless, there are innovative projects nowadays, like ELSA [1] and Batteries2020 [2], that are striving to give a second life to these batteries. Offering a second chance to these batteries would mean lowering their environmental impacts during their life cycle.

The end of an EV battery life is defined by the US Advanced Battery Consortium as a 20% drop of cell capacity from the rated value, or a 20% drop from rated power density at 80% depth of discharge (DoD) [3]. In other cases, the battery end of life can be considered achieved when its resistance has doubled in value. Yet, after being used in an EV, these batteries can still be useful in other applications and can be selected and rebuilt for a new purpose, such as Energy Storage Systems (ESS) for stationary applications [4].

In order to have a homogeneous battery selection issued from various first lives, it is important to characterize the cells of a battery pack with respect to State of Health (SoH). However, in this study the Incremental Capacity Analysis (ICA) was here used to give a more intimate diagnosis of the batteries, pursuing a more precise characterization of the cells or modules for the assembly of the second life battery. This refine selection means a more homogeneous battery, in which the cells would age similarly during the second life.

This paper is organized as follows. In the second part, a few diagnostic methods are presented and the feasibility of their use in second life applications is discussed. The third part presents the ICA as a diagnostic tool to determine with accuracy the battery DMs. The experimental procedure is detailed and the results are explained and compared to other studies. To further visualize the effects of degradation, the fourth part presents the results of a Hybrid Pulse Power Characterization (HPPC) test. The fifth and last part confirms the experimental results with a simulation toolbox for battery degradation called *'Alawa*.

---

L. Albuquerque · F. Lacressonnière · X. Roboam  
LAPLACE, Université de Toulouse, CNRS, INPT, UPS.  
31055 Toulouse, France  
e-mail: albuquerque@laplace.univ-tlse.fr, fablac@laplace.univ-tlse.fr,  
xavier.roboam@laplace.univ-tlse.fr

C. Forgez  
Roberval, CNRS, UTC.  
60319 Compiègne, France.  
e-mail: christophe.forgez@utc.fr

## 2 Diagnostic methods for second life batteries

There exist many diagnostic methods for Li-ion batteries, but some are better suited than others to characterize the cell for a possible second life. They mainly give as outputs the SoH in terms of capacity (1) or impedance (2) [3,5].

$$SoH(Q)[\%] = 100 * \frac{Q_{present}}{Q_{nominal}} \quad (1)$$

$$SoH(Z)[\%] = 100 * \left( 2 - \frac{Z_{present}}{Z_{nominal}} \right) \quad (2)$$

Where Q is the battery capacity in Ah and Z is the impedance in Ohms. Precise methods based on machine learning are employed in Battery Management Systems (BMS), but they track the battery usage since their beginning of life to estimate the SoH [6]. In a situation where the previous usage is unknown, these methods would lack precision or not be applicable due to the small sample or nonexistence of first life data. Other methods such as the electrochemical impedance spectroscopy have been proven to be precise and capable of determining the DMs occurring inside the battery [7], but it requires specialised equipment capable of exciting the cells in order to extract their reaction to the applied frequency spectrum.

Since Li-ion battery degradation has been proven to be path dependent [8], meaning that their first life will influence the longevity and performance during their second life, two batteries can present the same SoH but have different degradation patterns. That is why, for a second life application, a diagnostic technique such as the ICA can be better suited to determine these degradation patterns in a battery cell or module. This method can be applied with simple laboratory equipment such as a power supply or an electronic load. With this technique, it is possible to estimate the Loss of Lithium Inventory (*LLI*) and the Loss of Active Material (*LAM*) in the positive and the negative electrodes of a Li-ion cell. These DMs are a better representation of the battery first life when compared to a simple capacity measurement.

## 3 Incremental Capacity Analysis

### 3.1 Principle

The ICA and Differential Voltage Analysis (DVA) are two similar methods that give an intimate view of the electrochemical processes inside the cell. Many papers have been previously published on these methods, but most of them focus on the estimation of the SoH during the first life [9–11]. In [9], it is possible to see how the Open Circuit Voltage (OCV) plateaus, which represent the convolution of the phase transitions inside the electrodes when being lithiated

or delithiated, become peaks in the IC curve by applying equation (3) [9]. In which the tips represents the existence of just one phase in one of the electrodes.

$$IC = \frac{dQ_{cell}[Ah]}{dV_{cell}[V]} \quad (3)$$

Where  $dQ_{cell}$  is the variation in capacity with respect to the voltage  $dV_{cell}$ . As illustrated in [12], the effects of the DMs can be translated in a shift between the electrode potentials, in the case of *LLI*, or a contraction in the case of *LAM*, which can happen separately in each electrode (*LAM<sub>PE</sub>* or *LAM<sub>NE</sub>*). These changes in the electrode OCV curves are ultimately going to change the overall signature of the IC curve and the amplitude and shift of the peaks can be used to estimate said DMs.

In order to acquire the IC curve, it is necessary to measure the OCV for each State of Charge (SoC) value of the battery. However, to obtain this measurement, it is necessary to charge or discharge the battery with low currents. Lower currents improve the precision of the measurement by preventing high diffusion effects inside the electrode materials and thus the precision of the IC curve. These diffusion effects can mix the electrode phase transitions into one single indistinguishable curve, as seen in [13]. This study concludes that *C/6* is a good compromise between time and precision, but there are studies that go as far as *C/2*, like [14].

### 3.2 Experimental tests

Two NMC/Graphite Li-ion batteries were studied in this work. One module is composed of 12 cells connected in series which had been used in an EV. The second battery is a single cell similar to the ones used in the module and it has also been used in an EV. The nominal capacity of the module and the cell is equal to 25 Ah, according to the manufacturer's datasheet. Fig. 1 shows the cell used in the module.



**Fig. 1** A NMC/G Li-ion cell tested in this work. The module consists of twelve of these cells in series.

First of all, several charge and discharge cycles were done with the module and the cell in order to determine and compare their discharged capacities. During the tests,

they were both placed in a climate chamber at 25°C. The charge protocol used was a CC-CV profile, in which a constant current (CC) is applied until the battery has reached its maximum allowed voltage (4.2 V per cell), then the power supply switches to constant voltage (CV) regulation until a low current of  $C/50$  (0.5 A) is reached. The discharging process was stopped when the voltage across a cell was equal to 2.7V (the discharge voltage limit).

During the experimental tests, the twelve cells of the module were equilibrated (the voltage response for each cell was the same). Hence, in this study, the diagnosis of the module was based on one particular cell of the module (noted  $cell_m$  in this study). Fig. 2 shows the discharge curves in volts by ampere-hours for the  $cell_m$  and the single cell. As shown, the discharge capacity of the module is equal to 27.5 Ah whereas it is equal to 23 Ah for the single cell, evidencing that this last has a lower SoH. Moreover, it is clearly visible that the phase transition voltage plateaus and the overall curves shift towards lower voltages, which indicates ageing and a resistance increase. These observations support the interest in using the ICA and a resistance measurement as diagnostic tools to understand the DM effects on the single cell.

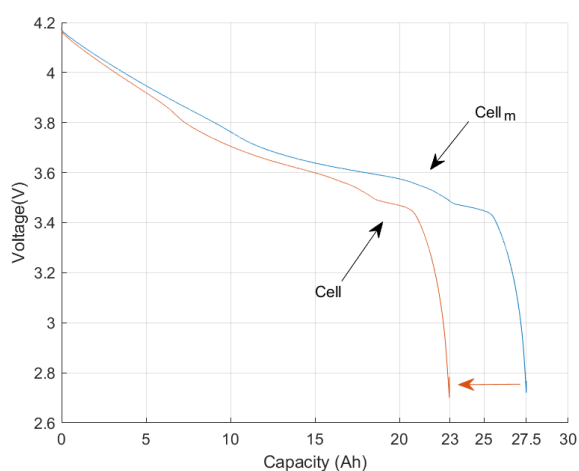


**Fig. 2** Discharge curves (with a C-rate of 0.2C) for a cell issued from the module and the single cell.

In order to obtain the DMs in both the  $cell_m$  and the single cell, the IC curve was plotted. As a first step to obtain the curve, a filtering on the voltage measurements is necessary before the derivative is calculated. As previously done in [15], the first filter applied to the voltage measurement was a moving average filter, giving a rough outline of the IC curve. Then the result was further smoothed by a Gaussian filter, in which the values of the averaging window are weighted with a Gaussian curve, where the center values have a bigger impact on the averaged value and the ones in the extremities have a lesser impact. The size of the av-

eraging window is increased to smoothen the curve until its peaks start decreasing in amplitude.

### 3.3 Interpretations

As previously said, the interest of the ICA is to analyze and identify the battery degradation phenomena intimately. To further understand and visualise the effects of ageing in the NMC/Graphite technology, the ICA method was applied to the single cell in order to compare its signature with  $cell_m$ . Fig. 3 shows both IC curves from a voltage measurement during the charging process. Several differences on the IC curves appear. These differences could be governed by ageing processes in the single cell.

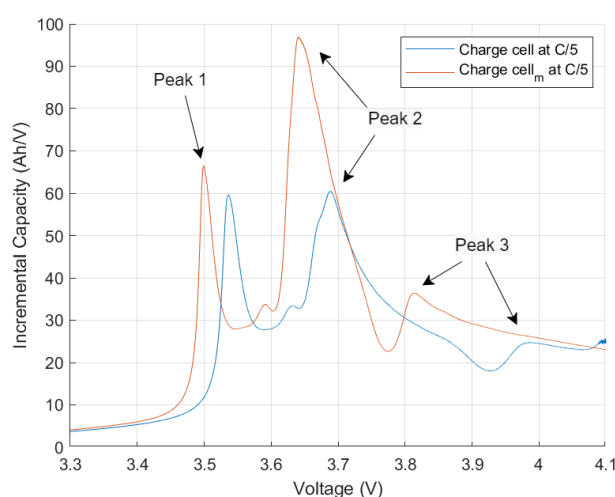


**Fig. 3** Comparison between the IC curve of  $cell_m$  (from the module) and the single cell.

The analysis of the IC curves demands an understanding of both the graphite and NMC electrodes behaviour simultaneously. Since the pair of curves presented on Fig. 3 comes from the charge profile, starting from the lowest voltages where the graphite is almost fully delithiated until the end of the first peak (2.7 V until 3.55 V for  $cell_m$  or 3.6 V for the single cell): the negative electrode passes from  $C_6$  to  $LiC_{72}$  (diluted phases), then  $LiC_{36}$  and finally transitioning to  $LiC_{18}$ . At this point, the mentioned graphite intercalation stages coexist, especially under high currents where diffusion effects are intensified.

The second big peak between 3.6 V and 3.75 V is mainly due to a NMC specific phase transition, where its structure changes from a hexagonal to monoclinic (H1 to M) lattice [16]. While so, the graphite transitions from  $LiC_{18}$  towards  $LiC_{12}$  corresponding to the end of the plateau between stage 3 and 2 in the graphite charge curve observed in the literature [17]. The third and last visible peak between 3.75 V and 4.1 V (shifted on the single cell IC curve) is primarily a

result of the last phase change in the graphite electrode from  $LiC_{12}$  to  $LiC_6$ . This transition is the longest of all (kinetically slower).

Due to the lack of a peak indicating the phase transition H2 to H3 (hexagonal to hexagonal accompanied by a rapid volume contraction) towards the end of the charge, reported in Ni rich NMC cathodes, the NMC cathode present in the batteries is presumed to have a relatively good reversibility and this is translated into a good overall stability of the electrode [18], so in a first moment,  $LAMP_E$  does not seem to be the main cause of ageing. However, the lower first peak (3.5 V) amplitude can indicate small traces of active material loss of the positive electrode  $LAMP_E$ .

Moreover, as a result of  $LLI$ , the cut off voltage (low SoC) of the positive electrode becomes higher as the lithium is consumed and it shifts both electrode potential curves away from each other. This means that at the end of a discharge or the beginning of a charge cycle, the positive electrode cannot reach lower voltage potentials due to the voltage limits (as in figure 8 from [19]). So, instead of having a strong peak between 3.6 and 3.75 V, its amplitude is considerably reduced. This indicates that  $LLI$  is the most prominent degradation mode at this stage of ageing. The consumption of lithium can also explain the overall shift of the IC curve towards higher voltages, since it is probably consumed during the thickening process of the SEI (Solid Electrolyte Interphase) layer.

### 3.4 C-rate influence on the ICA

A study to further understand the influence of the C-rate on the IC curve was also conducted. Fig. 4 shows IC curves plotted for several C-rates. The applied filters follow the same rule as explained in section 3.2. It was checked that the peak amplitudes were not equally affected by the charge or discharge regimes. The influence of the C-rate on the IC curve can be explained by the difference in kinetics of charge transfer and diffusion reactions in the electrodes for the different current values. This corroborates to choose a lower C-rate, in order to obtain an accurate IC plot. Hence, the choice of the C-rate has to be a compromise between the accuracy of the IC curve and the duration of the test for a rapid evaluation of the second life Li-ion batteries.

The analysis of two peaks from the IC curve (charge regime) for different C-rates was carried out and the results are summarized in Tab. 1. When the C-rate increases, the peak amplitudes are reduced and they shift toward higher voltages due to the voltage drop governed by the internal resistance. A reduction of peak areas is proportional to the number of exchanged amperes-hours during the charging process.

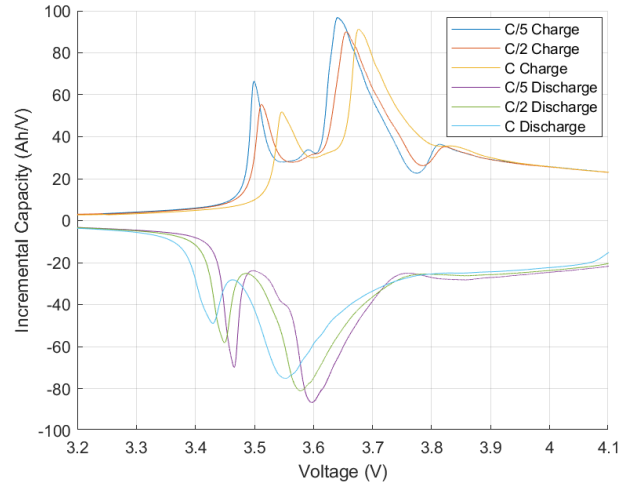


**Fig. 4** Comparison between different C-rates in charging and discharging modes for the cell<sub>m</sub>.

**Table 1** Comparison of peak amplitude and shift depending on the C-rates.

IC peaks for different C-rates in charging mode				
C-rates	1st peak: Amplitude	1st peak: Voltage	2nd peak: Amplitude	2nd peak: Voltage
0.2C	66.4 Ah/V	3.5 V	96.76 Ah/V	3.64 V
0.5C	55.4 Ah/V (-16.6%)	3.51 V (+11 mV)	89.91 Ah/V (-7.1%)	3.65 V (+14 mV)
C	51.8 Ah/V (-22%)	3.54 V (+46 mV)	91.22 Ah/V (-5.7%)	3.67 V (+35 mV)

## 4 HPPC profile characterization

As a complement to the ICA tests, a Hybrid Pulse Power Characterization (HPPC) test was carried out with both the module and the single cell in order to measure their internal resistances. One HPPC cycle profile consists on constant current charge and discharge pulses, followed by a 10% SoC constant current discharge and a 30 minute pause between cycles. The cycles are repeated until 10% SoC. One sequence of the HPPC profile is shown in Fig. 5 where several current rates were imposed at 0.1C, 0.2C, 0.5C, 1C, 1.5C and 2C. The duration of the pulses was fixed at 10 seconds and the internal resistance was calculated by Ohm's law. Fig. 6 presents the internal resistances measured for several SoC values. These values were calculated for cell<sub>m</sub> and the single cell for a discharge current of 1C. As depicted from Fig. 6, the single cell internal resistance is higher than the cell<sub>m</sub> in a ratio of 1.7, regardless of the SoC value. This internal resistance increase may be associated with ageing mechanisms taken place in the single cell and can explain the overall shift of the IC curve for the aged cell (Fig. 3), as mentioned previously, and may be linked mainly to the growth of the SEI layer.

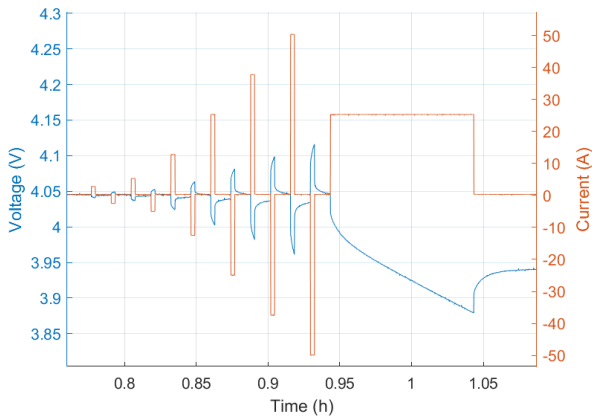


**Fig. 5** Current pulses and the voltage reactions during one sequence of the HPPC profile.

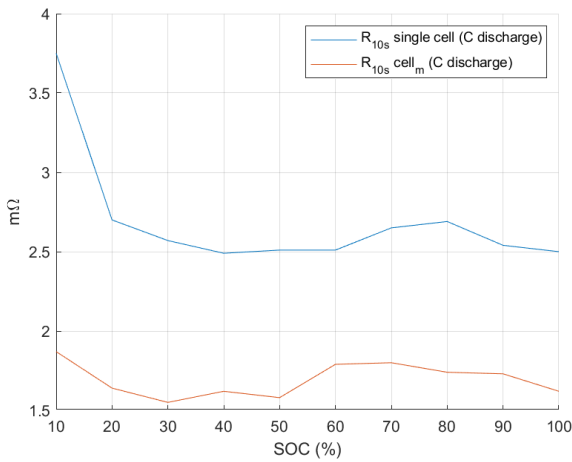


**Fig. 6** Internal resistance comparison between  $cell_m$  and the single cell.

## 5 ICA comparison with the *'Alawa* toolbox

Fig. 7 presents a comparison between the IC curves measured for  $cell_m$  and the single cell and IC curves obtained by using the *'Alawa* toolbox developed by Matthieu Dubarry et al. [20,21]. This software is able to simulate the DMs through a model based on individual electrode potentials, in which *LLI* is translated into a shift of the potentials and *LAM<sub>NE</sub>* and *LAM<sub>PE</sub>* are contractions of the electrode curves. The simulations are quantified based on a defined loss per cycle.

In order to simulate the degradation as close as possible to the experimental results, a few parameters such as the electrode ratio, the initial resistance and the SEI offset were chosen. This last one is responsible for the initial shift between the electrode curves, consuming lithium-ions. These parameters were modified until the obtained IC profile was close to the experimental one from  $cell_m$ . The same methodology was applied to simulate the DMs. The optimal result was found when the toolbox was set to simulate 0.032% of *LLI* and 0.01% of *LAM<sub>PE</sub>* per cycle during 500 cycles. These

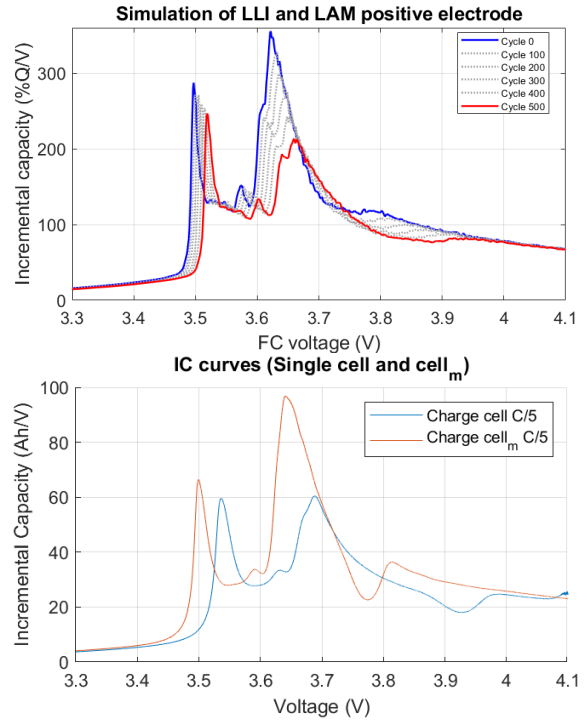


**Fig. 7** IC curves from *'Alawa* simulation of 0.032% of *LLI* and 0.01% of *LAM<sub>PE</sub>* per cycle (top) and IC curves from both the single cell and  $cell_m$  (bottom). %Q is the percentage of the initial battery capacity Q in Ah.

**Table 2** Comparison of the *'Alawa* simulations and the measurements. Note that *LLI* has been set to 0.032% per cycle and *LAM<sub>PE</sub>* and *LAM<sub>NE</sub>* were set to 0.01% per cycle.

DMs simulation and measured values				
Case	Degradation 1st peak	Degradation 2nd peak	Translation 1st peak	Translation 2nd peak
Experimental results	10.52%	37.83%	0.035 V	0.049 V
<i>LLI</i>	18.30%	44.27%	0.027 V	0.045 V
<i>LLI</i> + <i>LAM<sub>PE</sub></i>	14.10%	39.97%	0.022 V	0.038 V
<i>LLI</i> + <i>LAM<sub>NE</sub></i>	20.75%	40.54%	0.028 V	0.043 V

DMs result in a total of 16% of capacity loss and it is in accordance with the experimental value of 83.3% of SoH when dividing the capacity of  $cell_m$  to the aged one.

The total amount of capacity loss is due to *LLI* (16%), but the active material loss from the positive electrode has an influence on the IC curve as this electrode capacity has been reduced. Generally, the lower voltages are limited by the negative electrode and the higher voltage is limited by the positive electrode. Tab. 2 summarizes the simulations results with *'Alawa* and compares them with the real measured values.

The results presented in Tab. 2 show that with regard to peak degradation, the simulation with both *LLI* and *LAM<sub>PE</sub>* combined are the closest to the experimental results, also

supported by Fig. 7. The first peak is greatly reduced in the simulation with  $LAM_{NE}$ , as this peak is due to the first few phase transitions in the graphite, as mentioned in section 3. The peak translation in volts show close results in all of the cases, mainly due to the formation of the SEI as previously said. However, the differences are minimal, thus the peak amplitudes seem to be more adequate to judge the accuracy of the simulations.

## 6 Conclusions

In this paper, several tests were performed on a Li-ion module composed of 12 cells connected in series in order to estimate their state of health. These tests were also done with a single Li-ion cell. The capacity and internal resistance measurements allowed to distinguish a more important degradation for the single cell. An ICA was carried out to determine the degradation modes in the cell. It has been shown that the accuracy of the IC curves depends on the C-rate (amplitudes of the peaks decrease with the C-rate). To determine the degradation modes in the cell, the 'Alawa toolbox was used. A comparison between the IC curves (simulated and measured) showed that the major degradation mode in the cell is the loss of lithium inventory and the loss of active material of the positive electrode. In the future, this study will be extended in order to develop an experimental method, based on the ICA, to determine with accuracy (and rapidly) the degradation modes in Li-ion modules. This diagnostic method will be applied in order to have a homogeneous module selection to develop a second life battery.

**Acknowledgements** This work is funded by the B2LIVE project (Batteries de 2<sup>nd</sup> vie au Lithium Ion à Vieillessement caractérisé par Experimentation). This work has been supported by the OCCITANIE Region.

## References

1. ELSA project. <https://www.elsa-h2020.eu/Home.html>.
2. Batteries2020 project. <http://www.batteries2020.eu/>.
3. Ekilas Hossain, Darren Murtaugh, Jaisen Mody, Hossain Mansur Resalat Faruque, Md. Samiul Haque Sunny, and Naem Mohammad. A comprehensive review on second-life batteries: Current state, manufacturing considerations, applications, impacts, barriers potential solutions, business strategies, and policies. *IEEE Access*, Vol 7:pages 73215–73252, 2019.
4. Shijie Tong, Tsz Fung, Matthew P. Klein, David A. Weisbach, and Jae Wan Park. Demonstration of reusing electric vehicle battery for solar energy storage and demand side management. *Journal of Energy Storage*, 11:200–210, 2017.
5. Honorat Quinard, Eduardo Redondo-Iglesias, Serge Pelissier, and Pascal Venet. Fast electrical characterizations of high-energy second life lithium-ion batteries for embedded and stationary applications. *Batteries*, 5(1), 2019.
6. Nina Harting, René Schenkendorf, Nicolas Wolff, and Ulrike Krewer. State-of-health identification of lithium-ion batteries based on nonlinear frequency response analysis: First steps with machine learning. *MDPI Applied Sciences*, Vol 8(5), 2018.
7. Carlos Pastor-Fernández, Kotub Uddin, Gael H. Chouchelamane, W. Dhammika Widanage, and James Marco. A comparison between electrochemical impedance spectroscopy and incremental capacity-differential voltage as li-ion diagnostic techniques to identify and quantify the effects of degradation modes within battery management systems. *Journal of Power Sources*, 360(ISSN 0378-7753):301–318, 2017.
8. Zeyu Ma, Jiuchun Jiang, Wei Shi, Weige Zhang, and Chunting Chris Mi. Investigation of path dependence in commercial lithium-ion cells for pure electric bus applications: Aging mechanism identification. *Journal of Power Sources*, 274:29–40, 2015.
9. Elie Riviere, Ali Sari, Pascal Venet, Frédéric Meniere, and Yann Bultel. Innovative incremental capacity analysis implementation for c/lifepo4 cell state-of-health estimation in electrical vehicles. *MDPI Batteries*, 5(2), 2019.
10. Yuan Ci Zhang, Olivier Briat, Jean-Yves Deléage, Cyril Martin, Nicolas Chadourne, and Jean-Michel Vinassa. Efficient state of health estimation of li-ion battery under several ageing types for aeronautic applications. *Microelectronics Reliability*, 88–90:1231–1235, 2018.
11. Tiphaine Plattard, Nathalie Barnel, Loïc Assaud, Sylvain Franger, and Jean-Marc Duffault. Combining a fatigue model and an incremental capacity analysis on a commercial nmc/graphite cell under constant current cycling with and without calendar aging. *MDPI Batteries*, 5(1), 2019.
12. Christoph R. Birkl, Matthew R. Roberts, Euan McTurk, Peter G. Bruce, and David A. Howey. Degradation diagnostics for lithium ion cells. *Journal of Power Sources*, 341:373–386, 2017.
13. A. Fly and R. Chen. Rate dependency of incremental capacity analysis (dq/dv) as a diagnostic tool for lithium-ion batteries. *Journal of Energy Storage*, 29:101329, 2020.
14. E. Schaltz, Daniel-Ioan Stroe, K. Nørregaard, Lasse Stenhøj Ingvarsden, and Andreas Christensen. Incremental capacity analysis applied on electric vehicles for battery state-of-health estimation. *IEEE Transactions on Industry Applications*, 57:1810–1817, 2021.
15. Yi Li, Mohamed Abdel-Monem, Rahul Gopalakrishnan, Maitane Berecibar, Elise Nanini-Maury, Noshin Omar, Peter van den Bossche, and Joeri Van Mierlo. A quick on-line state of health estimation method for li-ion battery with incremental capacity curves processed by gaussian filter. *Journal of Power Sources*, 373:40–53, 2018.
16. Roland Jung, Michael Metzger, Filippo Maglia, Christoph Stinner, and Hubert A. Gasteiger. Oxygen release and its effect on the cycling stability of LiNixMnyCozO2(NMC) cathode materials for li-ion batteries. *Journal of The Electrochemical Society*, 164(7):A1361–A1377, 2017.
17. Rahul S. Kadam and Kishor P. Gadkaree. Thermodynamics of lithium intercalation in randomly oriented high graphene carbon. *International Journal of Electrochemistry*, 2017.
18. Hyung-Joo Noh, Sungjune Youn, Chong Seung Yoon, and Yang-Kook Sun. Comparison of the structural and electrochemical properties of layered li[nixcoymnz]o2 (x = 1/3, 0.5, 0.6, 0.7, 0.8 and 0.85) cathode material for lithium-ion batteries. *Journal of Power Sources*, 233:121–130, 2013.
19. Tobias C. Bach, Simon F. Schuster, Elena Fleder, Jana Müller, Martin J. Brand, Henning Lorrmann, Andreas Jossen, and Gerhard Sextl. Nonlinear aging of cylindrical lithium-ion cells linked to heterogeneous compression. *Journal of Energy Storage*, 5:212–223, 2016.
20. Matthieu Dubarry, Cyril Truchot, and Bor Yann Liaw. Synthesize battery degradation modes via a diagnostic and prognostic model. *Journal of Power Sources*, 219:204–216, 2012.
21. Matthieu Dubarry, M. Berecibar, A. Devie, D. Anseán, N. Omar, and I. Villarreal. State of health battery estimator enabling degradation diagnosis: Model and algorithm description. *Journal of Power Sources*, 360:59–69, 2017.